FEM EVALUATION OF SPRINGBACK AFTER SHEET METAL FORMING: APPLICATION TO HIGH STRENGTH STEELS OF A COMBINED ISOTROPIC-KINEMATIC HARDENING MODEL

Francesca Campana – Dip. di Meccanica e Aeronautica, Università di Roma "La Sapienza", Italy
Luca Cortese – Dip. di Meccanica e Aeronautica, Università di Roma "La Sapienza", Italy
Filippo Placidi – Centro Sviluppo Materiali S.p.A., Roma, Italy

ABSTRACT

One of the most relevant drawbacks concerning the use of new generations of HSS and UHSS, like Dual Phase (DP) and TRansformation Induced Plasticity (TRIP), is the larger amount of springback with the respect to traditional low carbon steel grades. It makes die set up more time consuming and reduces the design phase efficiency due to the inadequate accuracy of the Finite Element (FE) codes in the prevision of the final shape of formed parts made of such materials. To face this problem it is necessary to quantify this phenomenon for new steel grades and improve numerical tools. Among the different approaches that can be followed to improve the Finite Element Analysis (FEA) of HSS the most promising one concerns with the development of improved constitutive material models, able to better predict HSS behaviour.
This paper aims to present the results related to the application on HSS sheet metal forming of a combined isotropic-kinematic hardening model, that has been specifically implemented and calibrated by means of an explicit FEA code.

KEYWORDS

Sheet metal forming, Explicit FEA, Isotropic-kinematic hardening, Model calibration by "inverse approach".

INTRODUCTION

In comparison with other low carbon steels HSS main advantages are higher tensile strength and forming aptitude [1,2]. The first characteristic allows weight reduction of structural parts, without decreasing crashworthiness and fatigue strength. Formability mainly enhances the capability of forming together complicated parts saving, for instance, the cost related to the assembly phase. Nevertheless, stamped components such as automotive outer and inner panels mainly ask for dent resistance and rigidity, not tensile strength. Concerning denting, specific steel grades have been developed such as bake hardening, while rigidity is strictly dependent to panel shape, thickness and Young modulus. New HS steel grades allow obtaining bake hardening effects comparable to that of low carbon bake hardening steel and could be potentially applied to parts requiring dent resistance capability. The surface quality of such steel grades is generally not compliant with external panel requirement, even if study on the application of DP grades (i.e. DP 450) to skin panels and some industrial applications can be found.
One of the most important drawbacks related to the extensive application of HSS and UHSS is the accurate prevision and compensation of the springback phenomena [3].
The springback is more pronounced for UHSS than for other steel grades due to the adoption of lower thickness and higher non linear plasticity of such materials. In practice the die set up becomes more difficult and panel shape design may ask for more trial and error loops.
Usually Finite Element Analysis (FEA) of stamping processes helps in reducing shape design efforts, but the springback evaluation is one of the most difficult phase also for common grades but

HOME

in case of HSS often lower accuracy is achieved due to their different plastic behaviour. More in details, it has been experienced a change in compliance during loading and unloading in plastic regime [4] and a pronounced Baushinger effect [5].
This paper presents some results achieved within a RFCS research project that aims to quantify the role of the material behaviour in HSS springback occurrence, to improve its prevision and to enable guidelines for the use of these materials in the autobody design. More in details it concerns with the application of a combined isotropic-kinematic hardening model with the aim of improving springback estimation of HSS stamped panels. The adoption of such model has been done to take into account during plastic deformation not only hardening behaviour but also Baushinger's effect. In such way the final stress distribution can be evaluated with more accuracy, improving also the springback analysis results. This model, although already implemented in implicit FEA software, is still missing in explicit codes which are used in sheet metal forming [6,7]. For that reason a material user subroutine has been developed to include it in LS-Dyna.
In the next sections, after a brief introduction of the mathematical theory of the model, how the material model calibration has been faced and carried out on four HSS, provided by the research project, is widely discussed. Then some test cases and validations are presented to discuss the results achieved with the proposed model.

1. MODEL THEORY AND CALIBRATION

The implemented hardening law is a proper combination of isotropic and kinematic hardening rules. In particular yield is reached on the generalized Hill's yield surface described by the function:

$$f(\sigma_{ij} - \alpha_{ij}) - \sigma_s = 0 \tag{1}$$

where σ_s is the current yield stress, σ_{ij} the deviatoric part of the stress tensor and α_{ij} the deviatoric part of the back-stress tensor. This tensor takes into account the Bauschinger's effect, shifting the centre of the yield surface.
Equation (1) can also take into account material anisotropy introducing the L, M, N, F, G, H Hill's constants [8]. In the next applications we refer to the formulation without material anisotropy due to the fact that the adopted HSS present a r value between 0.9 an 1.1.
Backstress tensor is incrementally updated through the formula:

$$d\alpha_{ij} = \frac{C}{\sigma_s}(\sigma_{ij} - \alpha_{ij})\, d\varepsilon_p - \gamma\, \alpha_{ij}\, d\varepsilon_p \tag{2}$$

ε_p represents the effective plastic strain, while C and γ represent two material constants, to be defined by experimental tests, together with other two parameters, A and b, that are necessary to describe the hardening law according to the Voce's exponential law:

$$\sigma_s = \sigma_s^0 + A(1 - e^{-b\varepsilon_p}) \tag{3}$$

This model has been implemented as a material user subroutine of the LSDyna970 solver.
Material parameters A, b, C, γ can be given as parameters through LS-Dyna input file in the user material card. Young modulus, Poisson's ratio, material density, yield stress and anisotropy constants (if important) are also required.
The validity of this user subroutine has been checked out by means of various simulation runs performed with built-in LS-Dyna material models (e.g. Power Law Isotropic Plasticity, Kinematic Plasticity Model) and compared with others that have been made using user subroutine adapted with the same theoretical models. Since comparison showed no differences, the correctness of the implementation is granted.

A, *b*, *C* and γ are parameters able to described the behaviour of a specific material, so a calibration procedure must be defined to assess their values for each material. The model is incremental and non-linear in the respect of the strain path, due to the fact that we are describing the plasticity field, for this reason the assessment must be done by means of an error minimisation between experimental and numerical data according to a calibration procedure called "inverse approach" [9,10,11]. Three steps are required to obtain the material constants:

1. *Experimental test definition.*
2. *Finite Element modeling of the test.*
3. *Minimisation procedure set up.*

1. Experimental test definition. It must be able to shown the material behavior in the respect of the isotropic-kinematic model: to well captured Bauschinger's effect it has to be a cyclic tensile-compressive test on sheet metal forming. A cyclic three point bend test on a sheet metal specimen has been defined to avoid buckling occurrence. Figure 1 shows the experimental arrangement.

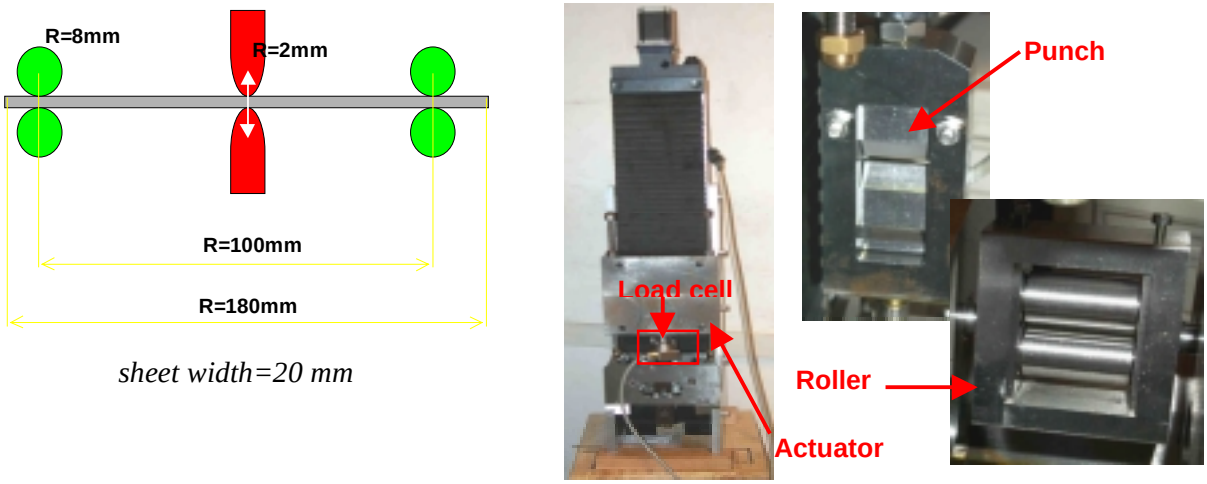

Fig. 1 – Experimental set up for model characterization

A rectangular specimen, 180x20x1 mm, is simply supported by roller constraints at the ends and loaded in the middle by an appropriate actuator. The actuator can be displacement controlled to perform bending-unbending cycles. To reduce friction on supports a system of bearings has been designed to realize the rollers, they can rotate along the sheet width direction. By this arrangement the contact lines between specimen and rollers change during all over the test. Friction is reduced by lubrication and no plastic strain arises because the sheet is free to slide along the roller.
The punch stroke range is [+ 30. –30] mm. Tests are made controlling punch displacement with constant speed (usually 1 mm/s). Punch stroke versus displacements is acquired during test by means of proper measurement devices. This curve represents the reference behavior to be matched by the minimization procedure that must evaluate the user subroutine parameters.
Figure 2.A shows an example of such curve, the cyclic behaviour is analysed on 5 quarters, according with the idea that this field of strain path better agrees with forming load conditions.

HOME

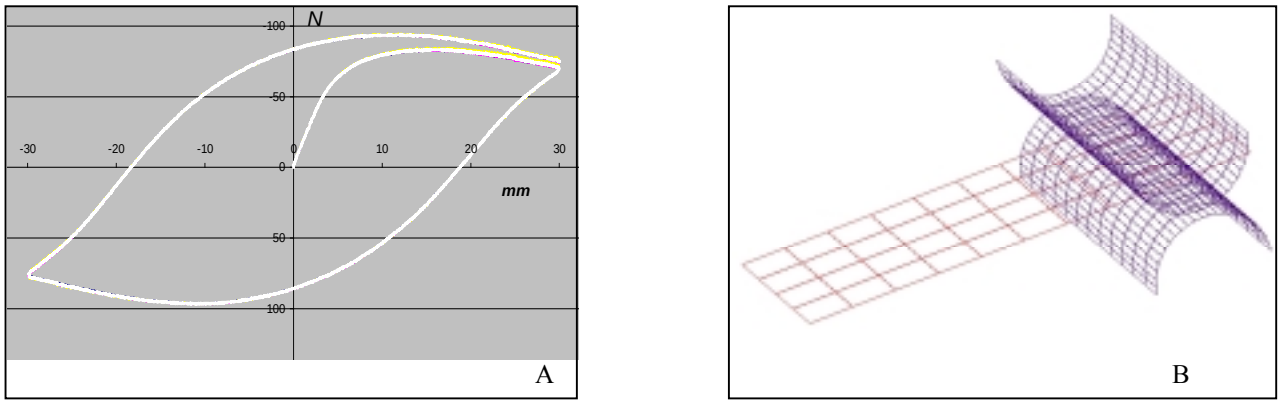

Fig. 2. A) Load-Displacement curve; B) FEA model of the experimental test

2. Finite Element modeling of the test. Its definition must allow the match between experimental and numerical results. It consists of an half specimen with one roller (figure 2.B). Sheet is modelled with fully integrated shell elements and exploits symmetry to reduce computing time. Many improvements in mesh pattern have been made run after run as the consequence of result analysis:

- early models were meshed with 1 element through width which gave quite inaccurate results; the cause was an in plane cross-sectional curvature that could not be "captured" by only one element;
- the number of elements along the length and the number of layers through thickness are tuned so that a further refinement does not produce any sensible improvement.

The specimen length is not equally to half specimen (90 mm) but smaller (61.5 mm), this was made to avoid inertial problems of a part, that one outer from the roller, that does not contribute to the phenomenon we want to study.
Friction has not been taken into account. The difficulties of a proper estimation of friction coefficient as a matter of fact leads to a greater approximation than neglecting it. Nevertheless experimental tests are made with good lubrication.

3.The minimization procedure. It assesses material constants by means of an optimization algorithm that looks for the mean square errors between the experimental cyclic curve and the numerical one. It has been implemented to allow an automatic research of the optimal parameter set. Starting from a first guess set of parameters, an iterative procedure links together FE calculations with an optimisation algorithm able to find an improved set of parameters.
The program can: (i) write the LS-Dyna input file at each iteration; (ii) excerpt the numerical results (force reaction and nodal displacements); (iii) rebuild the load-displacement curve; (iv) resample force and displacement at the same points of the experimental curve; (v) evaluate the quadratic norm among experimental and numerical data; (vi) compute a new set of parameters by means of an optimisation algorithm; (vii) evaluate the convergence between the current and the previous set of parameters and decide if the computation must be updated or stopped.
Two minimisation algorithm were implemented: the Leverberg-Marquardt and the simplex method. The first one was soon abandoned due to the fact that local numerical instabilities of the FEA load-displacement curve made quite difficult the convergence of the procedure. In many cases the objective function started to jump across the minimum without moving straight to it. Simplex method, on the contrary, is more reliable in finding an improved solution in each test case.

2. MATERIAL MODEL CALIBRATION

The calibration procedure has been applied to four types of HSS: two Dual Phase steel (named DP600_315 and DP600_313), a Transformation Induced Plasticity one (named TRIP700) and an HSLA one (named HSLA340).
The experimental tests were run with 4-5 replications for each rolling directions (0°, 90°, 45°) to assess anisotropy effect. This effect seems to be not so relevant: TRIP700 shows the greatest differences changing the rolling direction but the effect can be considered negligible (figure 3.A).

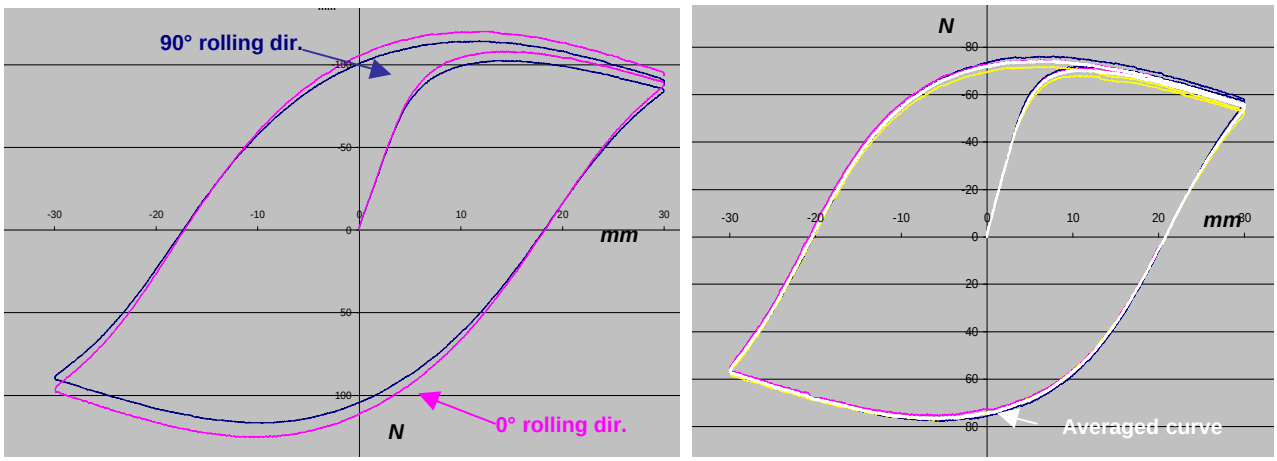

Fig. 3. A) TRIP700: experimental results changing rolling direction;
B) HSLA340: 0° direction, replicated tests

The scatter among the replications is quite small: figure 3.B shows the curves related to HSLA340 (0° rolling direction), the material that shows the highest dispersion.
Figure 4 summarises all the averaged curves, to perform a clear comparison among the different materials.
Unfortunately, a first run of the minimisation program did not give satisfactory results due to the fact that during unloading the slope of the experimental curves does not follow the same at the first loading step (that is equal to E). This behaviour has been already studied [12] and it has been assumed to cause unstable results during the optimisation procedure in correspondence of two different first guesses: in one case a good agreement is obtained in the unloading phase but not in the hardening part, in the other the hardening part description improves but it does not replicate the loading-unloading steps. To avoid this problem, two new degree of freedom have been given to the model, adding *E* and the initial yield stress as new material parameters. With this change the numerical curve fits better with the experimental data in all the areas and not only in one specific part.

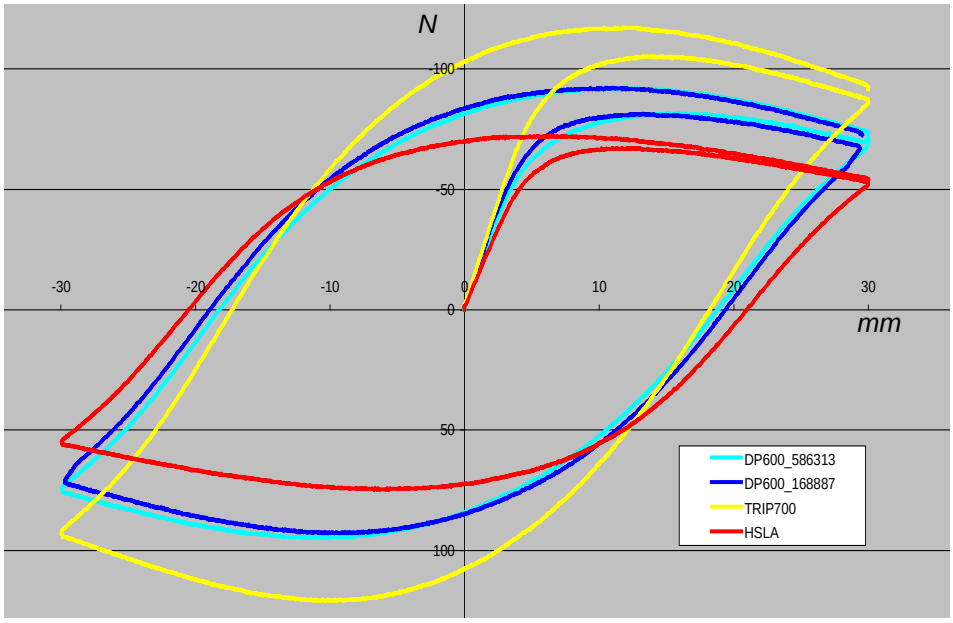

Fig. 4. Experimental results: averaged anisotropy curves

As a general procedure we decided to run the calibration in the respect of two different first guesses as shown in table 1. The first guess #1 gives more importance to the isotropic part of the model while the first guess #2 to the kinematic components. In this case the final Young's module is always greater than that one of the other first guess, so we generally assume as definitive the final values related to first guess #2.

Parameter values for averaged curves						
	E (MPa)	**σ_y**	**A (MPa)**	**b**	**C (MPa)**	**γ**
First guess #1	200000	*Material value*	400	21	5000	100
HSLA	152938	287	96.8	15.3	5405	193
TRIP700	178775	464.5	350.3	15.1	5224.9	103.1
DP600_315	157831	353.1	382.1	7.1	6557.6	141.6
First guess #2	200000	*Material value*	50	25	15000	135
HSLA	172397	261.1	44.1	27.5	15166.9	156
TRIP700	195023	483.4	51.4	24.8	16105.1	129.8
DP600_315	176714	342.6	46.4	25.7	18409.5	133.7
DP600_313	162674	358.7	51.5	26.1	16883.6	132.5

Table 1. Calibration parameters for anisotropy averaged curve

3. APPLICATIONS

Different basic test cases have been performed to compare the proposed combined model with the standard power law formulation. Figure 5 shows the TRIP700 and DP600_315 load-displacement curves achieved from the calibration parameters obtained with First Guess #1 and #2 in comparison with the experimental data (blue curve) and the Krupkowsky's law (white curve). In the case of DP600 the white curve after the first unloading becomes quite dissimilar from the experimental data, while the combined model with both optimal solutions (first guess #1 and #2) presents a better agreement. In the case of TRIP700 the maximum load conditions are always quite similar in both

the models, greater difference is shown during unloading phases. The results of figure 5 demonstrate that Krupkowsky's material model is not able to describe multiple cycling load paths.

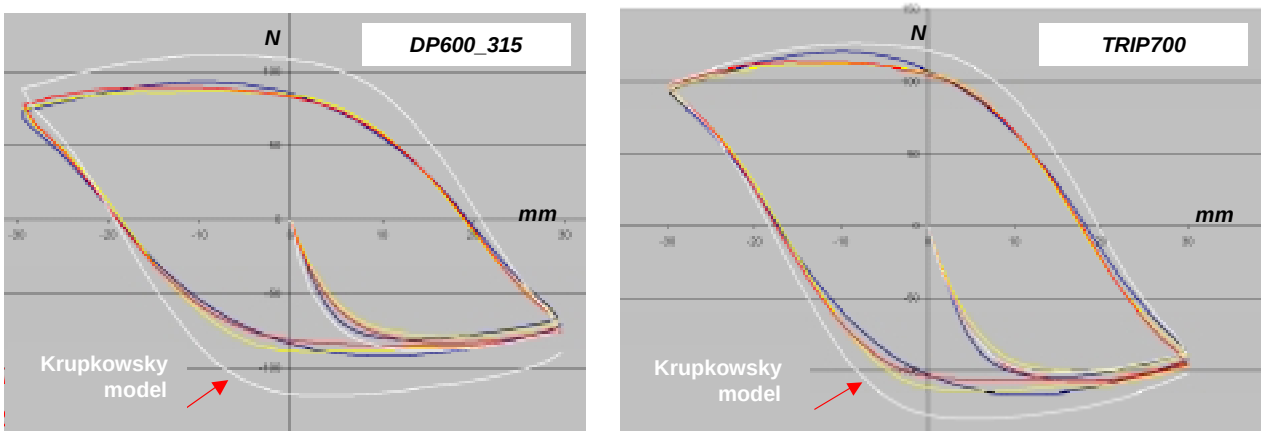

Fig. 5. Krupkowsky's model response to cyclic loading

The calibrated model has been applied also to different forming cases, comparing the final springback solution with both experimental ad other standard model FEA. Generally speaking, standard simulations assess a springback displacement smaller than the experimental one while the combined model partially fills the gap improving the solution. For instance applying the model to an unconstrained cylindrical bending, as defined by Numisheet'02 benchmark, the difference in the final displacement of the flange between experiment and FEA is always about 4%, while for TRIP steel using Krupkowsky's law it is about 14%. Table 2 summarises these results while figure 6 shows the distance adopted as springback (SPBK) measure. Notice that at the end of stamping the final value of the distance between the edges was 73 mm.

Springback			
	Experimental	**Krupkowsky**	**Combined model**
TRIP700	106.0 mm	90.4 mm	102.0 mm
DP600_315	101.5 mm	94.1 mm	98.4 mm
Krupkowsky parameters			
	TRIP700	DP600	
K	1306 MPa	990.3 MPa	
n	0.24	0.188	
Combined model parameters from first guess #2			

Table 2. Springback results of cylindrical bending

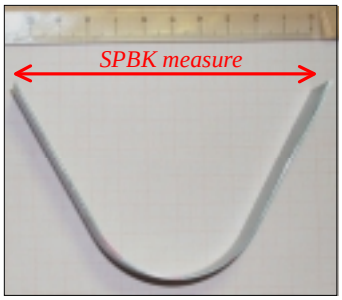

Fig. 6. Cylindrical Bending

To completely validate the model a more complex component was considered; to this aim, a roof panel has been adopted as industrial case of the research programme (figure 7). This panel is hydroformed starting from a DP600_315 blank 0.8 mm thick, next it is trimmed to obtain the final figure (cyan shape in figure 7). The Blank shape is 1160x750 mm, the maximum forming pressure has been 300 bar, and the blankholder force 2000 kN.

The validation plan comprises the measure of the strain field and of the final shape after trimming on the real component and finally their comparison with FEAs results obtained with the standard and the proposed model.

The strain measurements have been performed by CSM by means of a Camsys system; figure 8 on the left shows the measurement area, 40 x 40 mm, and the results (on the right). At this stage the trimmed component was not available yet. Despite of this lack of information the numerical

HOME

simulations have been performed anyway, and the springback after trimming has been evaluated by comparing the numerical results only.

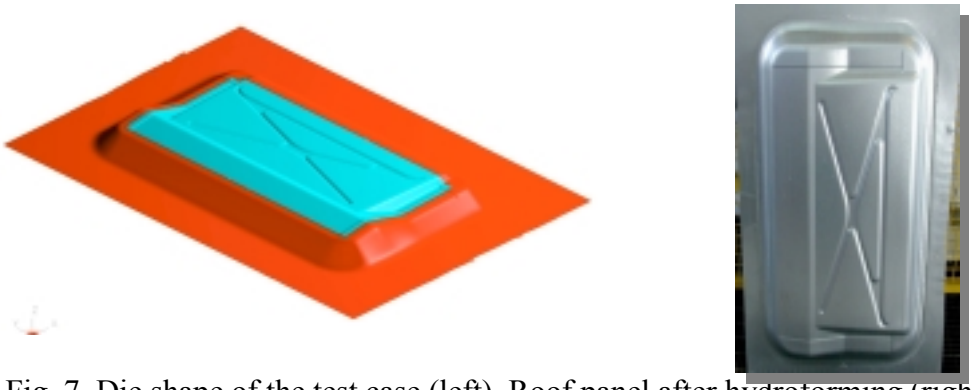

Fig. 7. Die shape of the test case (left). Roof panel after hydroforming (right)

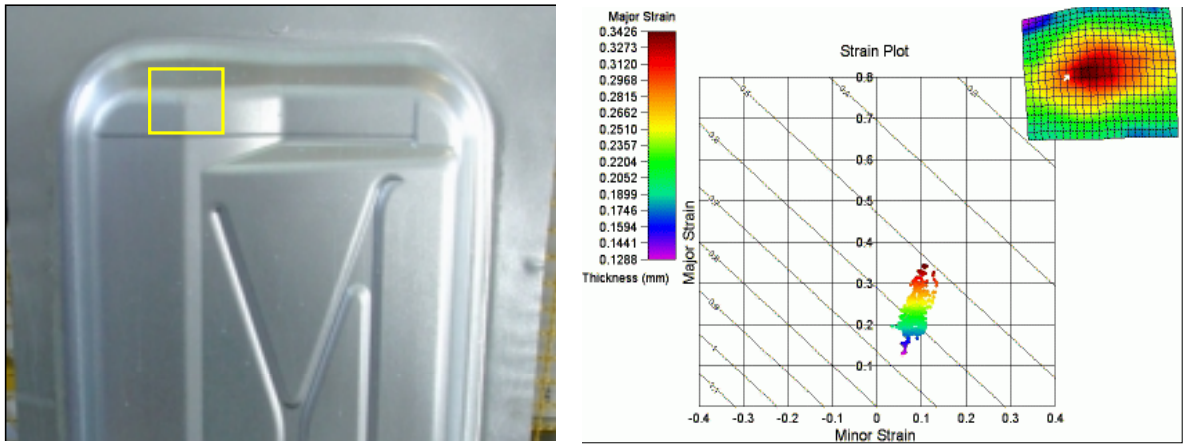

Fig. 8. Strain measurement

From the experimental measurements, the maximum final thinning is near to 37%. The standard Krupkowsky model reaches a value of 25% versus the 29% of the combined model solution.
Figure 9 and 10 show the vertical displacement after springback, for the Krupkowsky and the combined model respectively.

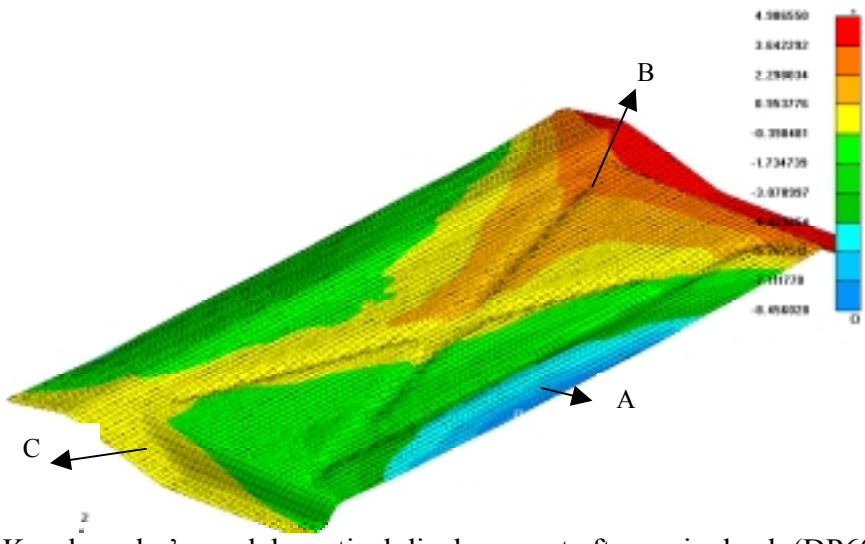

Fig. 9. Krupkowsky's model: vertical displacement after springback (DP600_315)

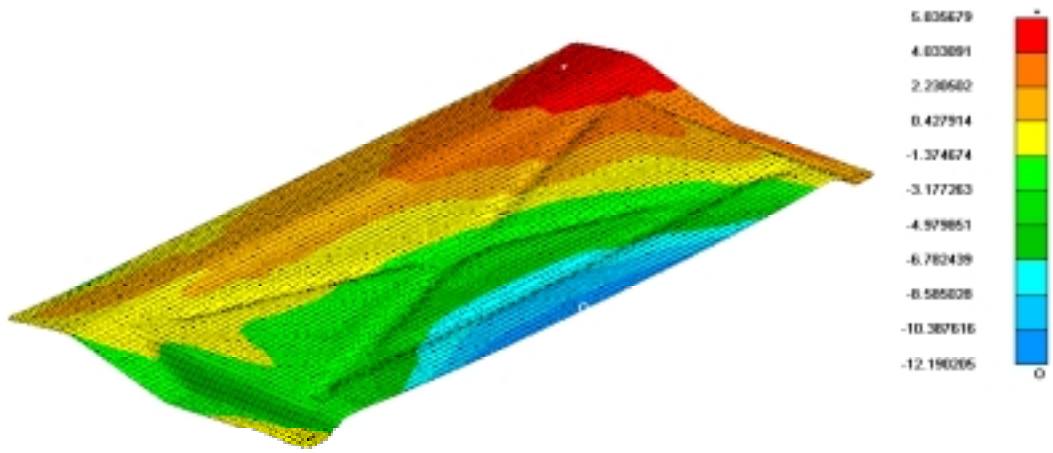

Fig. 10. Combined model: vertical displacement after springback (DP600_315)

The combined model confirms a more realistic aptitude to springback than the standard model. In region A, that is shown in figure 9, the maximum displacement is increased from 8.45 mm to 12.19 mm. In region B the maximum value is quite similar but the combined model localises the distortion in a more un-symmetrical way. Also in zone C there are some differences: the combined model amplified a small wave, depth of about 3 mm (gradient from yellow to green), not detectable on the standard model.

4. CONCLUSION

In HSS springback occurrence represents the major defect after stamping and FEA tools still miss in accuracy in predicting it, usually allowing a satisfactory evaluation of the component final shape but not of the total amount of the displacement. This makes more difficult the die design optimisation when dealing with HSS. In this paper the implementation in a explicit code (LS-Dyna), of a combined hardening model (isotropic and kinematic) to improve the springback results has been presented. In fact HSS during plasticity show different types of non–linearity such as change in compliance and Baushinger's effect. The proposed model takes into account this effect by means of a kinematic hardening formulation.
The model has been calibrated on different HSS by means of an inverse approach. The adopted experimental test consists of a tensile-compressive cyclic three point bending. The cycle has been performed two times plus a quarter.
Several test cases have been done to assess the quality of the results. First of all the calibration cyclic test has been compared with a standard FEA simulation performed by using a Krupkowsky's law: the combined model always fits better the experimental results, specially during unloading.
The second test case consists in evaluating the springback of rectangular blank stamped according to unconstrained cylindrical bending: the combined model underestimates the experimental results with an error less than 4%, for any material tested, while the Krupkowsky's model gives errors greater than 10%.
The third test case concerns with a roof panel made by hydroforming. Also in this case the combined model shows greater springback occurrence than the standard model, confirming the trend already experienced. From the experimental point of view the part trimming is still missing, nevertheless the strain measurements on a specific area of the panel shows a final thinning of about 37%; the standard model evaluates it about 25%, while the proposed model gives 29%.

Finally we can affirm that the combined hardening model is able to improve the sprigback evaluation of HSS without affecting the stamping results in comparison with other models.
The next research actions will be devoted to the experimental springback measurement on the component by using a reverse engineering system, allowing for a quantitative comparison with the model results.

REFERENCE

[1] E. Doege, S. Kulp, C. Sunderkotter, *"Properties and Application of TRIP steel in sheet metal forming"*, Materials technology, Steel Research.

[2] Manabu Takahashi, "*Development of high strength steels for automobiles*", Nippon Steel Technical Report no. 88, July 2003.

[3] A.M. Streicher, J.G. Speer, D. K. Matlock, "*Forming response of retained austenite in a C-Si-Mn high strenght TRIP sheet steel*", Steel Research 73, 2002, No 6+7, pp 287-293

[4] R. Cleveland, A.K. Ghosh, "*Inelastic effects on springback in Metals*", IDDRG2000, 21st Biennal Congress – Ann Arbor, Michigan, USA, June 2000

[5] Takeshi Uemori, Tatsuo Okada, Fusahito Yoshida, *"FE analysis of springback in hat-bending with consideration of initial anisotropy and the Bauschinger effect"*, Key Engineering Materials Vols. 177-180 (2000) pp. 497-502.

[6] K. M. Zhao and J.K. Lee, "*Springback prediction using combined hardening model"*, IBEC2000, Detroit, Mi, USA, October2000, SAE edition.

[7] Gau Kinzel, *"A new model for springback prediction in which the Bauschinger effect is considered"*, Int. J. of Mechanical Sciences, 43, 2001, 1813-18326.

[8] R. Hill, *"The mathematical theory of plasticity"*, Oxford University Press, 1950.

[9] K. M. Zhao and J.K. Lee, "Estimation of material properties from cyclic bend test", IBEC2000, Detroit, Mi, USA, October2000, SAE edition.

[10] F. Yoshida, M. Urabe and V.V. Toropov, *"Identification of material parameters in constitutive model for sheet metals from cyclic bending tests"*, Int. J. Mech. Sci. Vol. 40, Nos. 2-3, pp. 237-249, 1998, Pergamon.

[11] R.Mahnken, E.Stein, "A unified approach for parameter identification of inelastic material models in the frame of the finite element method", Comput. Methods Appl. Mech. Engin. 136 (1996) pp. 225-258.

[12] F. Morestin, M.Boivin, *"On the necessity of taking into account the variation in the Young modulus with plastic strain in elastic-plastic software"*, Nuclear Engineering and Design 162 (1996) 107-116, Elsevier.

HOME